A novel method for predicting site dependent specific rain attenuation of millimetre radio waves

Walther Åsen, Terje Tjelta

***Abstract* — The use of millimetre radio communication systems has seen a remarkable increase in recent years. However, there remains a need for validation and improvement of millimetre propagation prediction methods for safe design and operation of the systems. At this high frequency range propagation related degradation is primarily caused by rainfall. The goal is an improved method for predicting specific attenuation due to rainfall. A general method for establishing the relationship between rainfall rate and specific attenuation is developed. Drop size distributions (DSDs) measured by a Joss distrometer are analysed, and the three climate classification parameters rain rate, DSD median, and DSD mode are used in the development of these new methods. These parameters are investigated as candidate classes to categorise drop size distributions. Categories of the classes are then established to improve the long-term DSD estimate. The typical long-term DSD is used to derive new prediction methods that are compared with observed attenuation. The influence of wind on the rainfall measurements is studied, and a corresponding correction is suggested, reducing the prediction error significantly. Testing of the three new methods using measurements at 40 GHz and 60 GHz shows noticeable improvement over the method recommended by the International Telecommunication Union (ITU) using measurements at 60 GHz at deep attenuation.**

***Index Terms* — Rainfall rate, millimetre wave attenuation, drop size distributions, propagation prediction methods.**

I. INTRODUCTION

Millimetre wave radio systems are now commonly available and used for communication links and for broadband access systems. A congested spectrum and an increasing demand for broadband services are presumably the main reasons. However, the systems themselves are also very attractive. They are small and easy to install, and have therefore become popular among operators. Millimetre technology is reliable, although degradation may happen due to propagation phenomena. Rain is the main problem and has to be appropriately accounted for to make the systems work satisfactorily.

For temperate climates, radio waves of frequencies higher than about 10 GHz become significantly attenuated in rain. Attenuation increases with increasing frequency up to about 90 GHz and remains at an almost constant level over the rest of the millimetre wavelength range. The number and size of raindrops in the atmosphere are the most important factors. When propagating through a population of raindrops the radio wave will also experience different conditions depending on the raindrop shape, and the results will therefore in general vary with the polarisation of the electromagnetic wave. The specific attenuation is usually predicted from three parameters: frequency, rain rate and polarisation, where the population of raindrops is represented by the single parameter: the rainfall rate [1].

The distribution of rain along the radio propagation path may be inhomogeneous. Heavy rain showers are usually confined to a smaller area than lighter rain, and the rain area, or rain cells, may in principle have any shape. If rainfall rate is measured only at a single point it is difficult to know enough about the structure of a rain cell at some distance away from the observation point. Even with several rainfall sensors along the paths, the non-homogenous nature of rainfall may lead to incorrect estimates of the specific attenuation. A short path is therefore necessary for measurement of specific attenuation.

At millimetre wavelengths (1-10 mm) it is noted that the radio waves and raindrops are of comparable sizes. For an evaluation of the specific attenuation for millimetre waves it therefore seems essential to establish the DSD for rainfall.

The main intent of this paper is to derive specific attenuation methods taking advantage of local DSD data. This is done by introducing new methodologies for establishing a local climate typical DSD; essentially it is an algorithm for sorting measured DSDs. Furthermore the paper contributes on the reasons for discrepancies between predicted and measured attenuation, applicable for the new prediction methods as well as other methods.

The paper presents rain attenuation modelling in Section II, with a focus on relevant aspects when DSDs are available. Section III presents the measurements of DSDs and other meteorological data, and 40 and 60 GHz short path attenuation. DSD categorisation and the development of a new specific attenuation method are discussed in Section IV. Section V compares the different new methods, and section VI discusses the implications of the new methods on availability predictions. The effect of wind as a cause for under-prediction is discussed in Section VII. The

Walther Åsen is with Norwegian Defence Research Establsiment, but was with the Norwegian Post and Telecommunications Authority when this work was done.
Terje Tjelta is with Telenor Research and Development, Norway.

DOI til publisert versjon / DOI to published version: 10.1109/TAP.2003.818005

conclusions in Section VIII point out that the new method is comparable or better than the method recommended by the radiocommunications sector of the ITU (ITU-R). It also concludes that a first order correction for the wind improves significantly the prediction accuracy for all the methods tested.

II. ATTENUATION MODELLING

As recommended by ITU-R [1] the specific attenuation in rain is calculated by

$$\gamma = kR^{\alpha} \quad \text{(dB/ km)} \tag{1}$$

where k and α are coefficients dependent on frequency, polarisation and drop canting angle, and R (mm/h) is the rainfall rate. The theoretical validity of this exponential model was thoroughly reviewed by Olsen et al. [2] and found to be accurate over a large range of frequencies including the millimetre range. The frequency and polarisation dependent coefficients used in the ITU-R Recommendation P.838-1 [1] were derived by Maggiori [3] using Mie-theory for small spherical drops, a point-matching technique for large ellipsoids, and the Laws-Parsons (L-P) DSD. Since the DSDs may well vary from climate to climate this paper compares observations against the ITU-R method and where the new methods use locally obtained DSDs.

It has to be underlined that the accuracy of Equation (1) and its parameters depend on the DSD used, i.e., that of L-P. Clearly this is implicitly also the case if direct measurement is applied to derive values for k and α. But the simple form of (1) makes it easy to establish and compare parameter values from different climates. The aim of this paper is to make use of Equation (1) and derive k and α through a simple categorisation of DSDs. The method derived is directly portable to similar climates, and of course, the methodology can be used wherever DSDs are available.

A. Macroscopic rain attenuation

A model is required for calculating the macroscopic rain attenuation from (single) raindrop extinction. The intensity of an electromagnetic wave penetrating a medium where the fractional change of the intensity is proportional to the penetration depth (i.e., the medium is homogeneous on the scale considered) satisfies a differential equation stated in several textbooks, see for example Jenkins and White [4]. The general solution is a negative exponential function, and using the usual nomenclature in rain propagation modelling and connecting it to summation of bins of a distrometer

$$\frac{I}{I_0} = e^{-\sum_i 1000 \cdot n(D_i) C(D_i) L} \tag{2}$$

where I/I_0 is the fraction of the intensity relative to the starting intensity, $C(D)$ (m^2) is the extinction cross section for a single raindrop of diameter D (m), L (km) is the path length, and $n(D)$ (m^{-3}) is the number of raindrops of bin i in a unit volume. The summation is done over all possible drop diameters.

Hence, the intensity of an electromagnetic wave that meets absorbing and scattering raindrops decays exponentially with path length.

The attenuation is $A=\log(e)10\log(I/I_0)= 4.343\Sigma 1000 n(D_i)C(D_i)L$ (dB), and the specific attenuation becomes

$$\gamma = \frac{A}{L} = 4{,}343 \cdot 10^3 \sum n(D_i) C(D_i) \text{ (dB/km)} \tag{3}$$

By assuming a drop terminal velocity (v), only dependent on the drop diameter, the number of drops per volume $n(D_i)$ in the interval i can be estimated from the number of raindrops observed on the area S over the time interval t at the ground by

$$n(D_i) = \frac{N(D_i)}{v(D_i)\, t\, S} \ (\text{m}^{-3}) \tag{4}$$

The basic rain attenuation for a short path then becomes

$$A = \gamma L \quad \text{(dB)} \tag{5}$$

where A (dB) is the path loss due to rain over the path L.

B. Single raindrop extinction

The single drop extinction cross section, $C(D)$, is the sum of a scattering cross section and an absorption cross section. Several methods exist for calculating the extinction coefficients of a single particle at millimetre wave frequencies, of which the Mie-theory [5] is the simplest assuming spherical raindrops. The Point-matching method can handle any drop shape [6], and is therefore capable of modelling more real drop sizes. The T-matrix method considers arbitrarily shaped dielectric bodies [7]. ITU-R discusses more methods in their Handbook of Radio Meteorology [8]. The advanced models allow calculation of extinction coefficients of drops of a chosen shape, and attenuation will then depend on the canting angles of the drops, as well as a model of the ellipsoidal form of the raindrops, and are therefore more exact.

In this paper both Mie-theory and T-matrix calculations were considered initially, where the T-matrix is considered accurate over various drop shapes and radio frequencies. The percentage difference between Mie-theory and T-Matrix for horizontal polarisation was calculated using software available from the European Space Agency on the Internet referenced by ESA [9], and is shown in Fig. 1. For the Mie-theory a drop temperature of 10°C was used. As noted for the frequencies used for the measurements, 40 GHz and 60 GHz, the differences are very small. It was

therefore considered acceptable to use the quickly obtainable results by Mie-theory for the comparison between previous research and the calculations of the new methods (see Section IV).

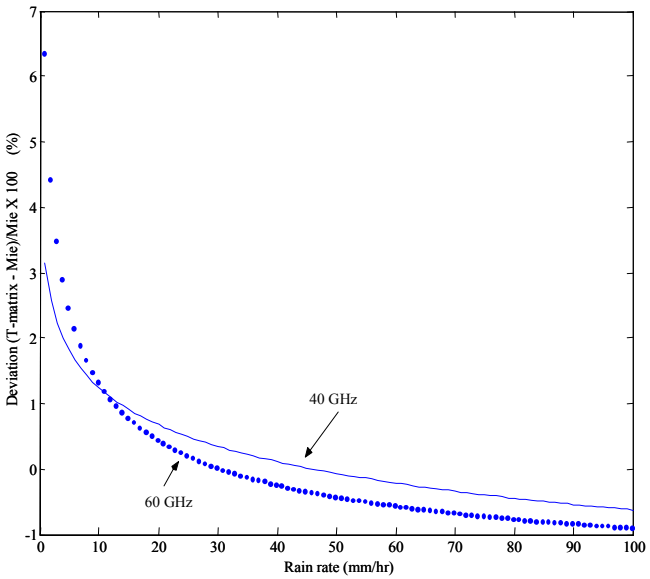

Fig. 1. The % difference between T-Matrix and Mie attenuation, at 40 GHz (-) and 60 GHz (.), for horizontal polarisation, and for the rain rate category distributions found in this paper

In principle, a method to adjust for canting angles could be used. However, the standard deviations in the linear regression estimates were of the same order of magnitude or larger than a difference due to a 45 degree canting angle. Thus, the influence by wind-shear caused varying canting angle is not used for assessing deviations of the attenuation method.

C. *Volume drop density*

The volume drop density *n(D)* is calculated according to Equation (4), from counts of raindrops onto a circular area of the distrometer. It is then necessary to use a model for the terminal velocity of raindrops as a function of drop diameter $v(D)$. The relationship is found by equating the gravitational force acting on a drop to the frictional force when it has reached terminal velocity. In practise the analytical expressions are adjusted by experiment, and the most quoted work is done by Gunn and Kinzer [10]. A fit to these data is given by Brussaard and Watson [11]:

$$v(D) = \begin{cases} 4.5D - 0.18, & 0.075 < D <= 0.5 \\ 4D + 0.07, & 0.5 < D <= 1 \\ -0.425D^2 + 3.695D + 0.8, & 1 < D <= 3.6 \end{cases} \quad \text{(m/s)} \qquad (6)$$

In the calculations the equation was extended for all drop diameters up to 5.5 mm. A comparison between this fit and the original data has been calculated and is found to be less than 1 % for drop diameters smaller than 4.2 mm. From 4.2 mm to 5.5 mm (the limit of the distrometer) the error ranged from 1 % to 10 %.

D. *Uncertainties in calculations*

Both the uncertainties in $n(D)$ and the uncertainties in $C(D)$ contribute to the inherent uncertainty of the model. The uncertainties in the extinction coefficients are mainly due to the shape of the raindrops, temperature, and canting angle deviations due to wind-shear.

The instantaneous size distributions that are measured vary significantly between samples that are commonly averaged over 10 seconds. The measured drop sizes are detected at the relatively small area (a circular area of 8 cm in diameter) of a distrometer that is situated at the receiver end of the propagation path. Volume estimates of equivalent uniform drop densities that are to represent the entire radio path are calculated from these point data.

E. *Fitting of data to parametric models*

In order to obtain stability over some time, a time series rain event is frequently modelled as a process where raindrops are distributed as for instance gamma or log-normal functions of (slowly changing) time varying parameters[12],[13]. By assuming that the parameters vary slowly and not significantly within a single rain event, one can categorise events by these parameters.

This paper uses another type of modelling to get around the problem of fluctuations. An average drop size distribution is obtained. The time average is assumed to also represent the average conditions for the propagation path. The long integration times is combined with sorting of the data in order to form a conditional distribution. Some physical constraint on the rain type should form the sorting criteria. In this paper the constraints have been rain rates, DSD medians and DSD modes.

III. MEASUREMENTS

A. *Set up of equipment*

A measurement set-up established at the Telenor R&D premises, Kjeller (11°02' E and 59°58' N), about 20 km North and East of Oslo, has been operated since 1993. Fig. 1 shows the 600 m radio path crossing a slightly inclined farming land. This part of Norway normally has a stable and cold inland climate during winter periods, fairly wet and foggy autumns, and fairly dry springs and summer periods occasional with heavy rain showers in the summer afternoons.

The measurements have been running over a long period. Data from May 1993 to September 1995 have been used in the analysis presented in this paper.

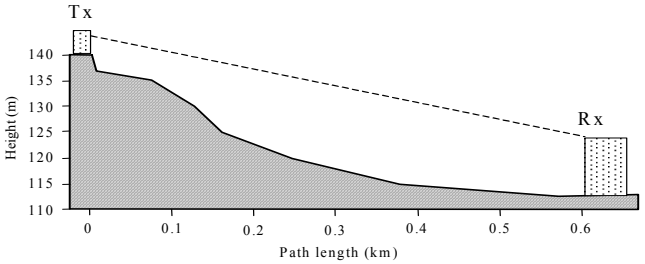

Fig. 2. Propagation path

Long-term attenuation measurements have been collected since May 1993 at horizontally polarised single frequencies of 40 and 60 GHz. The transmitters had horn antennas of about 8° beam widths and were located at the high end of the path (Tx). At the receiver end (Rx) similar horn antennas were used. Receivers with reflector antennas of 1.2° beam widths were added at a later stage to minimise ground reflections and to facilitate studies of the difference between narrow and wide beam antenna. Ground reflections may play an important role during periods with snow-covered ground. In fact, significant variation of the received signal level was observed receiving with the horn antennas [14]. However, these were significantly reduced when using parabolic reflector antennas. The receivers were partly made by Telenor R&D. Both the transmitter horn and receiver horn antennas were mounted inside a house behind a window (acrylic). Shields and fans have been installed to prevent snow from collecting on the reflector antennas.

The meteorological measurements include precipitation, air temperature, pressure, humidity, and wind force and direction. The precipitation is measured by two independent methods: the number and size of raindrops (a "Joss" distrometer), and the weight of accumulated water. The latter simply collects and measures the accumulated amount of water. Some oil and a non-freezing liquid are added to prevent evaporation and freezing. This pluviograph is particular useful during winter months, also because of its large circular collecting area of 20 cm in diameter. The circular collection area of the distrometer is 8 cm in diameter. The data series time resolution is one second for the radio attenuation time series.

The main characteristics of the measured items are listed in Table 1. All available data have been considered in quality checking of selected events. The study has been limited to the attenuation data obtained by the horn receivers in order to maximise number of events, since the receivers with reflector antennas were installed at a later stage. However, the latter data were used for validation of the horn antenna data. Also some meteorological data were used only for the quality checks. E.g., the weight pluviograph validated the total amount of rainfall deduced from the distrometer.

B. Selection of events

Events have been chosen where both attenuation and distrometer data are present simultaneously, and where the calculated rain rate from the distrometer exceeds 10 mm/h at least once during the event time series. The procedure includes all the measurements with rain rates higher than 1 mm/h. All events have been used for the analyses of DSDs. Events 1 and 5 of Table II could not be used for the attenuation comparisons shown in Figs. 6, 7 and 8. The reason for exclusion was that the events were partly contaminated by hail precipitation making them non-suitable for the comparison.

TABLE I
MAIN CHARACTERISTICS OF MEASURED ENTITIES

Measured parameter	**Equipment**	**Sampling period**	**Measurable range**
Attenuation 40 GHz Horn	Lab	1 second	40 dB
Attenuation 60 GHz Horn	Lab	1 second	40 dB
Attenuation 40 GHz Reflector	Lab	1 second	40 dB
Attenuation 60 GHz Reflector	Lab	1 second	40 dB
Rainfall rate	Aanderaa	1 minute	max. 240 mm/h
Accumulated precipitation	Geonor	1 minute	max. 600 mm
Dropsize	Distromet	10 seconds	0.35 to 5.5 mm
Temperature	Aanderaa	1 minute	-47 to 49°C
Wind strength	Aanderaa	1 minute	up to 60 m/s
Wind direction	Aanderaa	1 minute	0 to 360 deg.
Air pressure	Aanderaa	1 minute	920 to 1080 hp
Relative humidity	Aanderaa	1 minute	0 to 100 %

Table II presents a list of the events summarising the main features: ID is the event number. START TIME is start time of the event. STOP is stop time of the event. N is the number of observations with more than 1 mm/h of rain. Nw is the number of observations with wind less than 1 m/s and more than 1 mm/hr rain. WS is the maximum wind speed observed. MAX_R is the maximum rain rate of each event. These parameters have been included to characterise the events.

TABLE II
SUMMARY OF MEASUREMENTS.

ID	START TIME	STOP	N	Nw	WS	MAX_R
1	93 05 24; 14:45	15:45	62	2	8.8	67
2	93 05 24; 17:00	17:20	116	35	2.5	64
3	93 05 24; 20:30	21:15	195	0	4.2	19
4	93 06 12; 08:30	12:05	206	24	3.6	15
5	93 06 21; 11:45	12:15	113	0	4.6	55
6	93 07 12; 1500	16:00	78	0	5.5	21
7	93 07 15; 2015	20:53	162	38	8.1	23
8	93 08 06; 1630	17:30	168	6	4.9	51
9	93 08 09; 0915	09:45	113	0	4.9	27
10	93 08 09; 1000	13:00	565	0	4.5	23

ID	START TIME	STOP	N	Nw	WS	MAX_R
11	93 08 09; 2000	21:45	377	178	2.1	24
12	93 08 11; 1510	15:40	66	0	4.8	29
13	94 05 25; 1430	17:50	112	0	6.9	24
14	94 08 13; 1847	22:46	859	42	6.3	27
15	94 08 17; 1720	18:20	199	84	3.6	133
16	94 08 17; 1830	19:30	253	49	2.7	68
17	94 08 25; 1900	22:00	371	157	5.2	20
18	94 08 26; 0940	13:40	1312	252	4.5	22
19	94 08 27; 1534	23:41	846	98	6.1	18
20	94 09 10; 1100	11:45	89	0	7.6	80
21	95 05 31; 0035	04:30	807	705	1.3	26
22	95 06 11; 0730	08:30	263	36	4.9	81
23	95 06 17; 1750	18:10	55	4	2.8	127
24	95 09 03; 1123	15:15	629	0	5.5	44
25	95 09 04; 0410	06:10	462	84	3.9	43
26	95 10 18; 0145	02:15	107	0	8.5	82
27	95 10 25; 1556	18:00	85	0	7.5	10
28	95 10 27; 1440	18:30	783	0	6.9	33

IV. ATTENUATION PREDICTION METHOD BASED ON AVERAGED DSD

To derive the new prediction methods three steps are performed:

- establish an average DSD (that will be typical for the climate where the observations are taken) and by classifying the observed DSD into characteristic categories of a chosen class, denoted X,
- use Equation (3) to calculate per individual value of X the specific attenuation γ_X with the extinction coefficient C_X obtained by Mie-theory, and
- find k and α from linear regression on the logarithmic form of Equation (1), i.e., $\log(\gamma_X)=\log(k)+\alpha \log R_X$, where R_X is the rainfall for each value of category X contribution to the total rainfall rate.

Earlier results following this principle were published in [15], but in this paper a different approach is taken for the translation from rain rate to attenuation. Equation (1) is used, and the analysis is built on more data sets (28 events compared to 7 events in the earlier paper).

A. Choice of parameter classes

Either some sort of mathematical modelling or a categorisation process is necessary in order to make general hypothesis from physical observations of DSDs. In this paper simple parameters are used. These are the rain rate, the median and mode of the DSDs. Each of these parameters is analysed separately. The decision of which category (interval of a parameter) a measurement belongs to is made after each 10 second measurement. Fig. 3 illustrates extraction of the mode and median parameters. The corresponding rain rate R is calculated assuming spherical raindrops

$$R = \frac{1}{6St}\pi \sum_i N(D_i) D_i^3 \qquad (7)$$

where S is the surface area of the distrometer, and t is the measurement time.

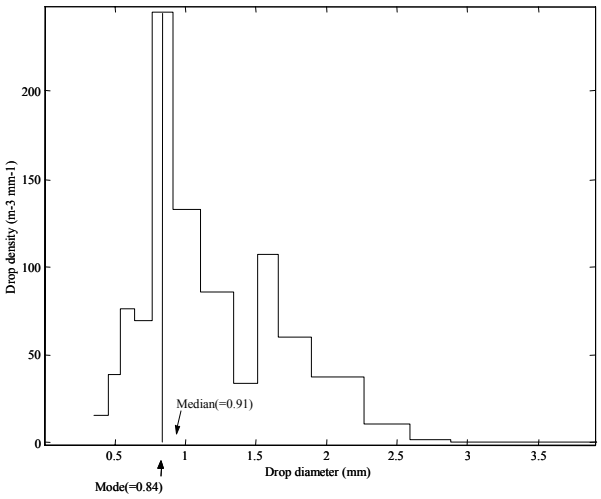

Fig. 3. A typical DSD

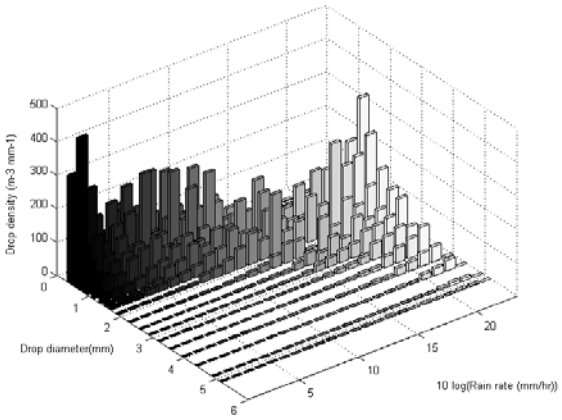

Fig. 4. Illustration of a DSD rain rate matrix, dependent on the rain rate parameter

B. Matrix formulation

The Joss distrometer measures a DSD every 10 seconds. The form of the DSD may vary a lot from sample to sample. When looking at a large number of DSDs, each point on the distribution will have a fairly large standard deviation.

A method is introduced which reduces the long time series of rapidly varying drop size distributions to parameter dependent distributions. If N is the number of raindrops, the description $N(t,D)$ is one element of a (usually large) matrix that spans all drop sizes D and times t, a (usually long) time series. The object is to reduce the large matrix to a smaller one of elements $N(X,D)$, which spans X and D, where X is some interval of a chosen parameter of the distribution, such as median, mode or rain rate. $N(X,D)$ is formed for

each parameter in question, i.e., $N(X_{median},D)$, $N(X_{mode},D)$ and $N(X_{rate},D)$ is formed.

Let $N(t,:)$ denote the distribution over the measured drop diameters at time t, and $N(X,:)$ denote the distribution over the measured drop diameters and over all category parameter values of class X. In order to calculate $N(X,:)$, each $N(t,:)$ is considered in turn. First the parameter value interval of $N(t=\text{t1},:)$ is found, say X=x1. This is repeated for all values of t, calculating a corresponding value of *N for* the category/group of X. Then the average is taken of all $N(t,:)$ which belong to the same category/group X=x1, and the result is stored in $N(X,:)$.

Fig. 3 shows one of the measured distributions $N(t,:)$, transformed to drop density in units of (m^{-3} mm^{-1}), where the mode and median are identified, contributing to the matrix shown in Fig. 4.

Fig. 4 shows the categorised average drop size density distributions for three years of data. The matrix is an example using rainfall rate, or rather 10 log$R$, as the parameter. For a given rainfall rate, the histogram (DSD) is shown along the drop diameter axis.

A large amount of 10 second measurements are required in order to get good estimates of the matrices. The variability for various rain types and events indicates that such measurements should typically be taken over several years. As well as calculating matrices for the mean number of raindrops $N(X,D)$, matrices containing the standard deviations of these means, $\sigma_N(X,D)$ have been obtained. In the detailed analysis not discussed here, $\sigma_N(X,D)$ has been used to confirm the significance of the obtained $N(X,D)$.

When reducing the data set to matrices the 10 second integrated distrometer data have been chosen, since this is the shortest integration time available. A longer integration time will increase the probability of significant changes of the measured attenuation during the period.

For the purpose of modelling the DSDs $N(X=\text{x1},:)$, without reference to attenuation, the matrix is transformed to drop density in units of (m^{-3} mm^{-1}) and fitted to a form of the shifted log-normal distribution found in Brussaard and Watson [11]

$$N(D) = N_0 \frac{1}{v(D)\,(D+s)\sigma\sqrt{2\pi}} e^{\frac{-(\ln(D+s)-\mu)^2}{2\sigma^2}} \quad (\mathrm{m^{-3}mm^{-1}}) \quad (8)$$

where shift s = 1 (mm) and tabulated values for the average rain rate and parameter values for rain rate categories are given in Table III. The errors introduced by the fit (in calculated extinction) are less than 10 % at 40 GHz, and less than 9 % at 60 GHz. The fit is done by first adjusting N_0 to the measured rain rate. A search is then done to find the combination of σ and μ which minimises the mean square error between the curves. The search step for each of the parameters was 0.01.

TABLE III
FITTED PARAMETER VALUES OF MEASURED RAIN RATE MATRIX FOR EQUATION (8)

Rain rate (mm/h)	N_0	μ	σ
1.1	1034	0.48	0.21
1.3	967	0.52	0.21
1.6	1214	0.51	0.22
2.0	1217	0.55	0.22
2.5	1441	0.55	0.23
3.2	1380	0.61	0.22
4.0	1403	0.66	0.21
5.0	1498	0.70	0.20
6.3	1537	0.74	0.20
7.9	1668	0.77	0.20
10.0	1801	0.81	0.19
12.6	1958	0.84	0.19
15.7	2128	0.87	0.19
19.7	1862	0.94	0.20
24.8	1724	1.00	0.21
31.5	1765	1.05	0.21
40.0	1973	1.08	0.21
50.1	1796	1.14	0.23
62.5	2068	1.16	0.23
79.6	2069	1.20	0.26
99.1	2377	1.21	0.28
125.3	2631	1.25	0.28

C. Model parameters calculated from DSD

Using Equations (3) and (6), $N(X,D)$ is used to calculate pairs of (R,γ), for each value of X.

Once these pairs have been established for each parameter value, they are used to find estimates for k and α of Equation (1). By taking the logarithms of both sides of Equation (1), and doing linear regression on $\log(\gamma_R)=\log(k)+\alpha\log(R)$, the coefficients are found (i.e., $\log(k)$ and α). These values are then representative for a long time average.

Separate estimates for k and α are obtained from each of the matrices of the parameters rain rate, median drop diameter and mode drop diameter.

For the rain rate matrix the rain rate parameter 10log$R$ used in the regression varies linearly between 1–19 (19 parameter bins), which corresponds to rain rates between 1-79 mm/hr. Thus 19 attenuation and rain rate pairs are used in the regression. Outside this range of the parameter the uncertainty in the matrix is large, the counts few, or a combination.

For the median and mode matrices the parameters are median diameter and mode diameter respectively, and the range of diameters used in the regression are between 0.35-1.89 mm. Outside this range the uncertainty in the matrices

have been large, the counts few, or a combination. Thus there are 11 bins for the parameters, i.e., pairs of attenuation and rain rate used in the regression.

Once the matrices are established, the parameters k and α are derived and attenuation as a function of rain rate predicted for any frequency of interest. The methods will be referred to as RATE, MEDIAN and MODE. This indicates each of the regressions using the rain rate, the median and the mode matrix, respectively.

Several authors have discussed the existence of multiple peaks in drop size distributions [16], [17]. It is suggested that the peaks may be due to an inaccurate calibration of the RD-69 distrometer [18], [19]. A more accurate calibration, given by the latter reference, is therefore used for the analyses in this paper.

V. Comparison of the Different Prediction Methods

The model described by Equation (1) with different values for parameters k and α may be compared for different rain rates at 40 and 60 GHz. Table IV shows the different values of k and α found, with and without wind correction in the categorisation process as described in Section VII. The regression coefficients found when calculating k and α range between 0.972 and 0.994 for the RATE method, between 0.968 and 0.996 for the MODE method, and between 0.924 and 0.988 for the MEDIAN method.

TABLE IV
CALCULATED VALUES OF PARAMETERS OF EQUATION (1) FROM DSD MATRICES

Method		**RATE**		**MEDIAN**		**MODE**	
Para.	Freq.	Wind corr.		Wind corr.		Wind corr.	
	GHz	No	Yes	No	Yes	No	Yes
k	40	0.33	**0.32**	0.31	**0.30**	0.34	**0.31**
α		0.94	**0.97**	0.97	**0.99**	0.94	**0.98**
k	60	0.81	**1.08**	0.66	**1.03**	0.82	**1.03**
α		0.75	**0.71**	0.81	**0.72**	0.73	**0.72**

Figs. 5a and 5b show the difference between the methods RATE, MODE, MEDIAN and the ITU-R method (New method minus ITU-R method). In Fig. 5 the ITU-R method is used with circular polarisation, since this gives the results most comparable to Mie-theory calculations for spherical raindrops. At 40 GHz the deviation is less than 0.5 dB for rainfall rates below about 50 mm/h, and at 60 GHz for rain rates up to about 35 mm/h. Above these rainfall rates the ITU-R method predicts less attenuation at 40 GHz and more attenuation at 60 GHz. Note also that the disagreement above about 20 mm/h rainfall rate shows, although small at 40 GHz, that the new methods predict more attenuation at 40 GHz and less at 60 GHz.

VI. Implications of the New Method on Availability Predictions

Figs. 6a and 6b show the distribution of measured attenuation compared to the ITU-R method. In Figs. 6, 7 and 8 horizontal polarisation is used throughout for the ITU-R method, since this is the polarisation of the measurements that are compared to the methods. The measured data were obtained at 1 s sampling rate, but here the plot shows the 10 s average aligned with the rainfall rate observations.

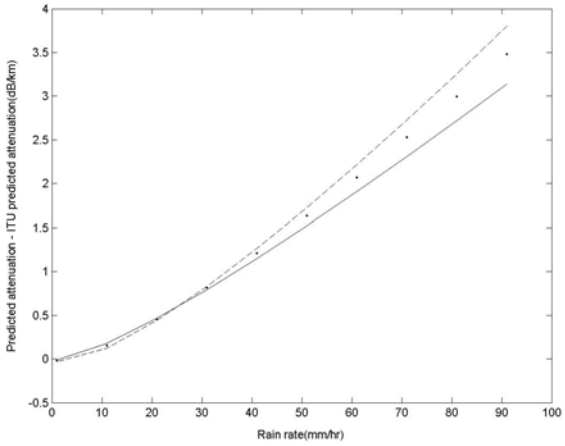

a) 40 GHz

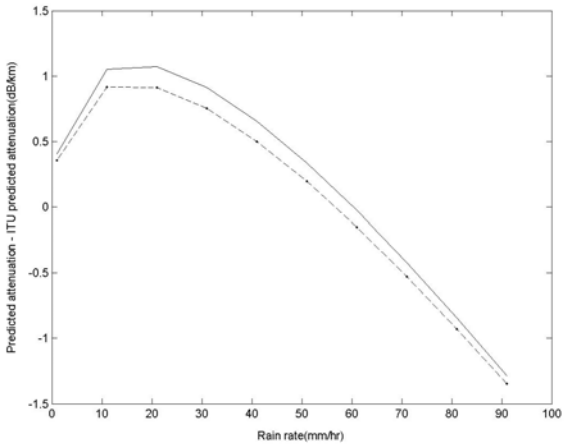

b) 60 GHz

Fig. 5. Curves showing the difference between the new prediction methods and that of the ITU-R (New methods minus ITU-R method) at 40 and 60 GHz rain attenuation for the range of rain rates 1-100 mm/h. '-' is RATE method, '- -' is MEDIAN method, and '.' is MODE method. The wind correction developed in Section VII has been applied

Deep attenuation events have been included. It is noted that the considered measurements represent a fraction of about 0.005 of the total time elapsed. In Figs. 6, 7 and 8 this number is used in the calculation of percentages of an average year, and is only an estimate, since the measurement procedure is focused on events, and not on long time uninterrupted data collection. For both 40 and 60 GHz, and over the range between 0.1 % and 0.002 % of the time, a big difference between the ITU-R method and measured attenuation is observed.

DOI til publisert versjon / DOI to published version: 10.1109/TAP.2003.818005

All the figures depict that there is a discrepancy between measured and predicted distributions. Merryweather-Clarke et al. [20] and Manabe et al. [21] have reported the same trend from similar short path experiments.

At high rainfall intensities it is reasonable to assume that there will be a discrepancy between observed and predicted values. A 600 m path results in an averaged attenuation observation, whilst the prediction is based on rainfall rate observed at a single point. Clearly more extreme values will be seen at one single point. Figs. 6,7 and 8 confirm large over-prediction of the highest attenuation. Furthermore, the higher the rainfall intensity, the more in-homogenous the rainfall, even over short paths.

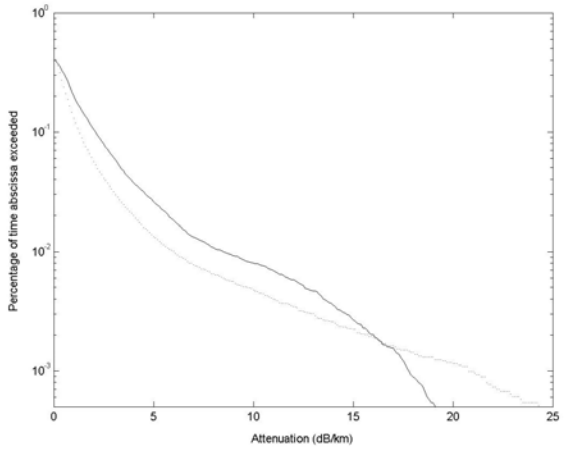

a) 40 GHz

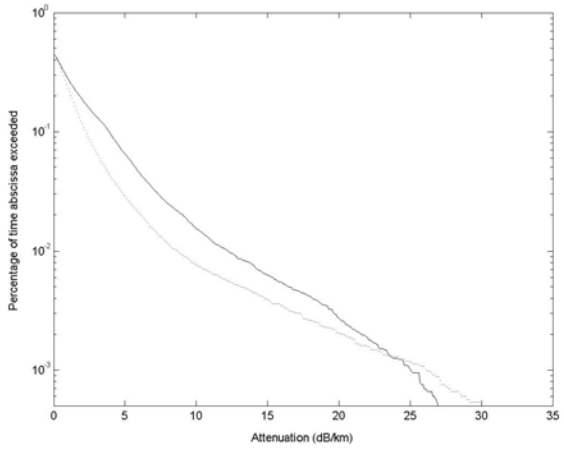

b) 60 GHz

Fig. 6. Predicted and observed attenuation distributions at 40 and 60 GHz: The ITU-R method ('.') and measured attenuation ('-'). The slanted rainfall modification developed in Section VII has not been used

At the intermediate and lower rainfall intensities there may be many reasons for the discrepancies. In the region from 0.1 % to 0.002 % of the time an under-prediction of attenuation is evident from Figs. 6, 7 and 8. One possible reason is that not enough small rain drops are accounted for as the Joss distrometer is not sensitive to drops of diameter less than about 0.35 mm. However, an estimate of the contribution of these small raindrops can be made assuming the exponential distribution of Marshall and Palmer [22], and applying Mie theory. According to this calculation, at 40 and 60 GHz, the raindrops not counted by the distrometer for rain rates above 1 mm/h account for less than 2 % of the total attenuation. Furthermore, one may believe that there is uncertainty in the count of small raindrops, particularly due to updrafts and downdrafts. If the calculation is repeated for the number of drops less than 0.7 mm, even this number contributes, at rain rates above 10 mm/hr, to less than 5 % of the total attenuation. The uncertainty in this number should therefore be considerable less than 5 %.

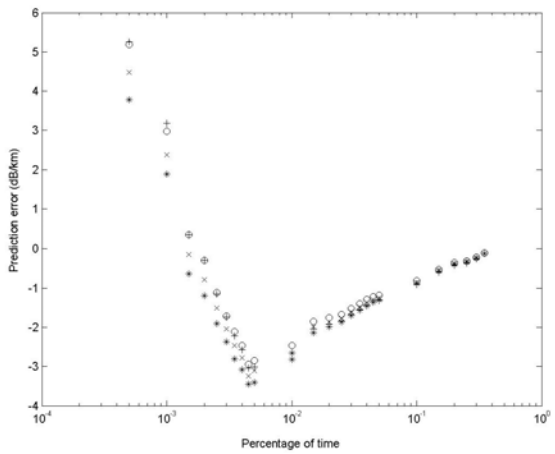

a) Slanted rainfall modification not applied

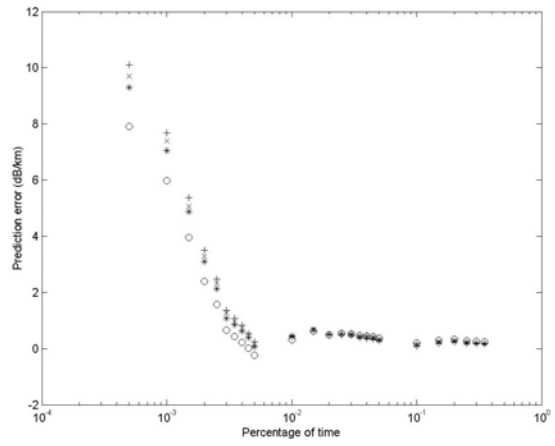

b) Slanted rainfall modification applied

Fig. 7. Predicted-measured attenuation for the different methods at 40 GHz: The ITU-R method ('o') the RATE method ('*'), the MEDIAN method ('+') and the MODE method ('x')

The under-predictions of attenuation found are up to 20 %. Other mechanisms have to be the cause. Sheppard and Joe [23] discussed the distrometer dead-time as a potential source for errors. This is due to the response time for the measuring equipment and the fact that the instrument cannot observe in a short period after each drop observation. Applying the correction suggested it has been

found that there is a very small underestimation of rainfall rate if the correction is not used. The figures indicate less than 5 % error.

By looking at the simultaneous horizontal wind data another potential explanation has been investigated; see the next section for further discussion.

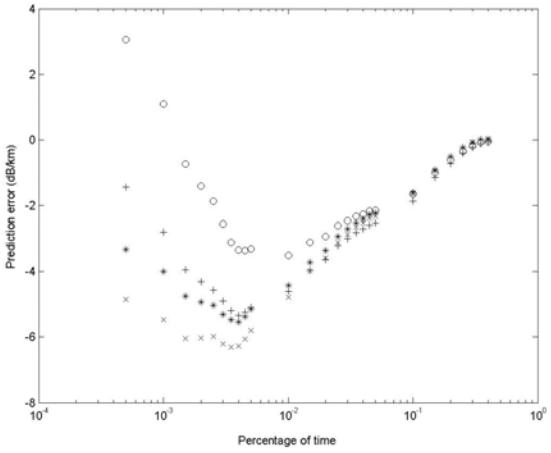

a) Slanted rainfall modification not applied

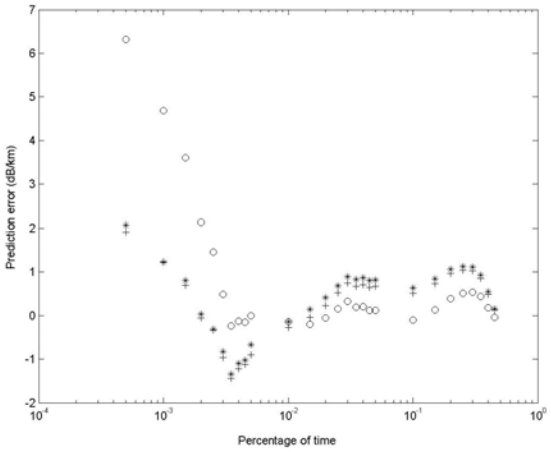

b) Slanted rainfall modification applied

Fig. 8. Predicted-measured attenuation for the different methods at 60 GHz: The ITU-R method ('o') the RATE method ('*'), the MEDIAN method ('+') and the MODE method ('x')

VII. CORRECTION MOTIVATED BY HORIZONTAL WIND DATA

The under prediction over a large range of the observed attenuation when using observed point rainfall rate, may have several reasons, but wind is possibly a prime source. As noted in Section I it is the number and sizes of raindrops in the atmosphere which cause attenuation. When observing the rainfall DSDs at ground level, and from one single point, it is important to use a good model to convert to volume particle density in the atmosphere above.

The presence of wind may cause several problems when comparing observed point rainfall rate with observed specific attenuation averaged over the 600 m path. The most likely problems are misalignment in time of rainfall event and the attenuation event, wrong estimate of volume particle density since the slanting rainfall will wet a larger area than vertical rainfall, and rain drop canting angles. Also wind-induced measurements errors are of some concern due to turbulence at the rain gauge, even likely to increase with smaller collecting area [24].

The attenuation variation due to canting angle is rather small, as also noted in Section II. For example at 40 and 60 GHz only 6-8 % difference, respectively, are estimated at R = 50 mm/h, between 0 and 90° angles. For the case of rain and attenuation event misalignment in time, a cumulative distribution should average out such effects.

Slanted rainfall could cause some discrepancy. Since terminal raindrop velocity varies with drop size, the DSD at the edges of the rainfall area may not be representative for the volume of interest when horizontal wind is present. In the leading edge of the rain the drops would be smaller, and in the lagging edge they would be larger than in the volume of interest. However, these areas are very small compared with the total rainfall area.

By looking at the individual drop-size dependent velocity resultant as a vector sum of the vertical terminal velocity governed by gravitational force and the horizontal velocity due to wind, a simple correction factor seems to work fine with the data. The model given in Equation (10) says that the amount of rainfall observed by the distrometer should be modified as a function of the cosine of the fall angle, i.e., the angle α the slanted path makes with the vertical

$$\alpha = \tan^{-1}\left(\frac{v_h}{v_v(D)}\right) \tag{9}$$

where v_h is the horizontal wind speed and $v_v(D)$ is the drop diameter dependent terminal velocity.
The modified rainfall R' is found by dividing the observed rainfall rate R by F

$$F(D) = \cos(\alpha) = \cos\left(\tan^{-1}\left(\frac{v_h}{v_v(D)}\right)\right) \tag{10}$$

By using the rainfall rate definition of Equation (7), and correcting the actual number of particles in the atmosphere for the underestimate at the rain gauge, a modified rainfall rate is obtained, R'

$$R' = \frac{1}{6St}\pi\sum_i N(D_i)D_i^3 / F(D_i) \tag{11}$$

In Figs. 6a and 6b an underestimation for the ITU-R method compared to measurement, of about 1-5 dB/km, is noticed, over a large availability range. Figs. 7a and 8a

show the difference between predictions and measurement for the same percentage availability ranges as for Fig. 6. When using R' instead of the rain rate as input to the attenuation functions, the difference is shown in Figs. 7b and 8b. Substitution of R with R' reduces significantly the prediction error for methods at low and intermediate availabilities. It seems proved that the distrometer underestimates the rainfall rate, although the fact that the drops follow a slanted path should not in itself lead to an underestimation. However, the correction works over a large range of time percentages, and physical explanations are probably related to horizontal wind.

It is clear that all of the methods are quite accurate for almost all availabilities at 40 GHz, and they perform equally well at the lower availability with over prediction. The ITU-R method seems to be excessively conservative in the high availability (low percentage) region at 60 GHz. The pessimistic performance of all the methods at high rain rates may be due to lower rain rate for part of the measured attenuation path.

The different DSD categories have a variable degree of success in estimating the average attenuation at different attenuation levels and at different frequencies, but the differences between the methods appear to be relatively small for our measurement site, especially when wind correction is made. This is clearly documented by Table IV, where there is little difference between the k and α values for the different methods when wind effects are accounted for.

VIII. Conclusions

Observed rain DSDs have been analysed with the aim of deriving a typical or time averaged DSD for the climate where the observations are taken. The DSDs have been categorised or sorted based on typical characteristics of the rain events. New specific rain attenuation prediction methods have been developed using the rainfall rate, the median, or mode drop sizes of DSDs as a parameter for the categorisation. This has been shown to be a very useful approach, as it gives comparable or better results than the ITU-R method when tested with observed attenuation data at 40 and 60 GHz.

Wind seems to have an effect on the estimated volume particle density in the atmosphere when estimated by the distrometer. If not corrected for, the measured attenuation may be noticeably larger than that predicted using the rain gauge data. A simple modification using the horizontal wind speed proved to correct much of the misalignment. Even not knowing the exact drop size distribution such a correction can be applied assuming a DSD, but the results might then become less accurate.

Future work is suggested for studying the relationship between observed long-term DSDs at the ground and the distributions of water drop and ice forming nuclei in the atmosphere. If DSDs are found to depend strongly on the constituents of the atmosphere, long term DSDs can be predicted from geographical maps of concentrations of nuclei.The physical impact of wind on rain gauges should also be investigated further, for example considering short rainfall observation times of minutes or shorter.

Having constructed typical DSDs for a climate, either based on measurements or modelling of the atmosphere, it will be possible to compare attenuation parameter values for different rain types from different sites of the world.

Acknowledgements

The authors are grateful for very useful discussions with Chris Gibbins, Rod Olsen and Sofus Lystad and suggestions made by the referees. The colleagues at Telenor R&D are thanked for help with the measurement site and discussions over the years.

References

[1] ITU-R Recommendation P.838-1, "Specific attenuation model for rain for use in prediction methods," *The Radiocommunications Agency of The International Telecommunications Union,* 1999.

[2] R. L. Olsen, David V. Rogers, and Daniel B. Hodge, "The aR^b Relation in the Calculation of Rain Attenuation," *IEEE Transactions on Antennas and Propagation,* vol. AP-26, no. 2, March 1978, pp. 318-329.

[3] D. Maggiori, "Computed transmission through rain in the 1-400 GHz frequency range for spherical and elliptical drops and any polarization," *Alta Frequenza,* vol. LN.5, Sept-Oct 1981, pp. 262-273.

[4] F. A. Jenkins and H. E. White, *Fundamentals of Optics*. 4.th ed., ISBN 0-07-032330-5, 1981, p. 746.

[5] G. Mie, "Beiträge zur Optik trüber Medien, speziell kolloidaler Metallösungen," *Ann.Phys.Leipzig*, vol. 25, 1908, pp. 377-445.

[6] T. Oguchi, "Attenuation of Electromagnetic Wave due to Rain with Distorted Raindrops," *J. Radio Res. Lab*., vol. 7, vol. 33, 1960, pp. 467-485.

[7] P. Barber and C. Yeh, "Scattering of Electromagnetic Waves by Arbitrarily shaped Dielectric Bodies," *Applied Optics*, vol. vol. 14, no. 12, December 1975, pp. 2864-2872.

[8] ITU-R, *Handbook on Radiometeorology*. The Radiocommunications Agency of The International Telecommunications Union, 1996. ISBN 92-61-06241-5

[9] OPEX, J. P. V. Poiares Baptista (ed.), "Reference Book on Radar," ESA WPP-083, *Proceedings of Second Workshop of the OLYMPUS Propagation Experimenters*, vol. 4, Noordwijk, The Netherlands, 8-10 November 1994.

[10] R. Gunn and G. D. Kinzer, "The terminal velocity of fall for water droplets in stagnant air," J. Meteorol., vol. 6, no. 4, 1949, pp. 243-248.

[11] G. Brussaard and P.A. Watson, *Atmospheric Modelling And Millimetre Wave Propagation*. Chapman & Hall. ISBN 0-412-56230-8, 1995, p. 329

[12] H. Jiang, M. Sano, and M. Sekine, "Weibull raindrop-size distribution and its application to rain attenuation," *IEE*

Proc.-Microw. Antennas Propag., vol. 144, no. 3, June1997*,* pp. 197-200.

[13] A. Maitra and C. J. Gibbins, "Modelling of raindrop size distributions from multiwavelength rain attenuation measurements," *Radio Science,* vol. 34, no. 3, May-June 1999, pp. 657-666.

[14] T. Tjelta, A. Nordbotten, and J. Kårstad, "Effects of Precipitation and Reflections from a Snow Covered Ground Measured at 40 and 60 GHz on a 600 m Experimental Link in Norway," Proceedings of ICAP'97, Edinburgh, 14-17 April 1997, pp. 2.234-238.

[15] W. Åsen and T. Tjelta, "Application of Measured Drop Size Distributions to Millimetrewave Rain Attenuation Modelling – A Study of Some Events," *Proceedings of the 8th URSI Commission F Triennial Open Symposium: Wave propagation and remote sensing*, 1998, pp. 67-70.

[16] M. Steiner, A. Waldvogel, "Peaks in Raindrop Size Distributions," *Journal of the Atmospheric Sciences,* vol. 44, no. 20, October 1987, pp. 3127-33.

[17] R. List and G. M. McFarquhar, "The Role of Breakup and Coalescence in the Three-Peak Equilibrium Distribution of Raindrops," *Journal of the Atmospheric Sciences,* vol. 47, no. 19, 1990, pp. 2274-2292.

[18] B. E. Sheppard, "Effect of irregularities in the diameter classification of raindrops by the Joss-Waldvogel disdrometer," *J. Atmos. Oceanic Technol.,* vol. 7, 1990, pp. 180-183.

[19] G. M. McFarqquhar and R. List, "The Effect of Curve Fits for the Disdrometer Calibration on Raindrop Spectra, rainfall Rate, and Radar reflectivity," *Journal of Applied Meteorology,* vol. 145, issue 3, 1993, pp. 180-185,

[20] N. Merryweather-Clarke, C. J. Gibbins, and D. N. Ladd, "The statistics of propagation on the 500 m millimetre wave experiment at Chilbolton," in Conf. Proc. of *10th International Conference on Antennas and Propagation,* 14-17 April 1997, Conference Publ., no. 436, IEE 1997, pp. 2.374-377.

[21] T. Manabe, T. Ihara, J. Awaka, and J. Furuhama, "The Relationship of Raindrop-Size Distribution to Attenuations Experienced at 50, 80, 140, and 240 GHz," *IEEE Transactions on Antennas and Propagation,* vol. AP-35, no. 11, November 1987, pp. 1326-1330.

[22] J. S. Marshall and W. McK. Palmer, "The distribution of raindrops with size", *J. Meteor. 5, 1948,* pp. 165-166

[23] B. E. Sheppard and P. I. Joe, "Comparison of Raindrop Size Distribution Measurements by a Joss-Waldvogel Disdrometer, a PMS 2DG Spectrometer, and a POSS Doppler Radar", *Jornal of Atmospheric and Oceanic Technology,* vol. 11, 1994, pp. 874-887.

[24] E. J. Førland(ed.), P. Allerup, B. Dahlström, E. Elomaa, T. Jónsson, H. Madsen, J. Perälä, P.Rissanen, H. Vedin, and F. Vejen, "Manual for operational correction of nordic precipitation data," Report no. 24, Norwegian Meteorological Institute, Oslo, Norway, 1996, p 64.